J. Comput. Appl. Res. Mech. Eng. Vol. 11. No. 2, pp. 351-364, 2022 *DOI: 0.22061/JCARME.2021.5860.1741*

Journal of Computational and Applied Research in Mechanical Engineering

jcarme.sru.ac.ir

SRTTU

JCARME

ISSN: 2228-7922

Research paper

Robust adaptive projection-based control of a constrained quadrotor with two manipulators

M. Mohammadi, R. Dehghani* and A. R. Ahmadi

Faculty of Mechanical and Materials Engineering, Graduate University of Advanced Technology, Kerman, Iran

Article info:

Article history:

Received: 19/08/2019

Revised: 06/08/2021

Accepted: 09/08/2021

Online: 12/08/2021

Keywords:

Constrained quadrotor,

Robust adaptive control,

Functional approximation technique,

Projection operator,

Wind force.

***Corresponding author:**

R.dehghani@kgut.ac.ir

Abstract

In this paper, a quadrotor with two manipulators constrained on a straight path is modeled and a robust adaptive controller is proposed for it. Adding two manipulators to quadrotor increases its capabilities and applications in industry. Here, these two manipulators are used to place the robot on a constraint path so that the quadrotor can perform monitoring operations more accurately, since the under-actuated quadrotor becomes over-actuated by these constrained manipulators and one can use this feature to accurately control the position of the robot. Reduced form of motion equations is derived for the constrained quadrotor and based on this a robust adaptive controller is proposed. The nonlinear terms in the dynamic model are approximated by basic functions with constant weights; and adaptive laws are designed by projection operator. Stability analysis is performed based on the Lyapunov theory. Evaluation of the presented controller is done by some numerical simulations. The simulation results showed that the robot tracks the reference path with bounded error in spite of dynamic uncertainties and wind force; and satisfies the considered constraints.

1. Introduction

Nowadays, as quadrotors have simple mechanical structure with high maneuverability, they are one of the preferred types of unmanned aerial vehicles (UAVs). This aerial vehicle has four motors whose propulsion thrust is generated by their propellers. Since a quadrotor has six degrees of freedom and four actuators, it is considered as an under-actuated robot. Also, the main problem is its low payload capacity. The quadrotors will be suitable for monitoring the traffic, pipeline and weather, as well as search and rescue operations and other diverse applications. Hence, these robots have received a lot of attention from many researchers all around the world. The dynamic modeling and simulation of quadrotors have been done by many researchers [1-3]. Additionally, multirotor helicopters have been investigated extensively [4] as a potential platform for such tasks because they are capable of hovering close to the ground, which is necessary for observing ground targets. Linearization of the dynamic model of quadrotor

using Taylor series approximation method has been presented in [5].

For the flight control of quadrotors, many methods have been proposed. One of these controllers is the proportional-integral-derivative (PID) control. This controller is designed and used for position and orientation control of the robot [6-10]. Many studies have been done on the stabilization of the quadrotor under external disturbances. For example, the external constant disturbances have been estimated using the Lyapunov functions and the validity of this method has been proved by experiments [11]. Recently, much attention has been paid to the use of nonlinear control methods for the flight control of quadrotors such as feedback linearization, fuzzy logic, sliding mode and back-stepping controller. Feedback linearization is used for controlling quadrotor [12-14]. Sliding mode control has been used for altitude control of a small helicopter in [15]. Also, the sliding mode control is used for controlling the movement of quadrotor [16-18]. In many studies, the steps of back-stepping controller with the proof of stability are presented [19-22]. Also, the performance of the back-stepping and sliding mode controllers for the robot's motion control were compared by Nadda and Swarup [23], and according to their simulation results, sliding mode controller functioned better.

Recently, the quadrotors are designed for advanced tasks due to their simple structure and high activity. Design, modeling and control of the interaction of a quadrotor with the environment are introduced by Sanchez et al [24]. In this area, some studies have addressed robust takeoff and landing of the quadrotor [25], quadrotor ball juggling [26], cooperative grasping and transport [27, 28], flipping [29], flight through narrows and perching on inverted surfaces [30], landing on moving platform [31, 32], and ensembles of aerial robots [33].

Adding two manipulators to quadrotor increases its capabilities. The application of quadrotor with two manipulators can be considered in different ways. This robot is able to use two manipulators in grasping and dynamic shipping, or moving along the surface by contacting two manipulators with that surface. Quadrotors with two manipulators are introduced in Yu and Ding's study [34]. The dynamic modeling of this robot, derived by using recursive method and trajectory linearization control of the robot on vertical surfaces, was proposed. Yu and Ding studied an optimal planning strategy [35]. Also, dynamic modeling and control motion of two armed quadrotors for wall-climbing mode and flying-walking locomotion are presented in Yu and Ding's study [36, 37]. In previous studies related to the control of quadrotors with two manipulators, the control law dependent on accurate information of nonlinear terms in the dynamic equations and the uncertainties of these terms were not considered.

In this paper, a quadrotor with two manipulators is considered such that the manipulators are constrained by a path. In order to conduct accurate monitoring of a path such as the high voltage lines, the robot must be resistant to external disturbances. Hence, in this paper, in order to overcome this challenge, the quadrotor with two manipulators constrained on the path has been proposed. Robust adaptive control design of the constrained quadrotor is one of the main contributions of this paper. The novelty of this article is that in designed controller, the nonlinear terms are estimated by functional approximation method and then the adaptive laws are designed by projection operator. The efficiency of the proposed controller and the robustness of motion in the presence of the model uncertainties and the external disturbances, are shown by some simulations.

2. Dynamical modeling of robot

The considered quadrotor with two manipulators is shown in Fig. 1. In this robot, the rotational axes of the propellers are parallel and the propellers, positioned opposite to each other, rotate in a direction reverse to the rotation of the coupling propellers. The main body of the robot has a square frame with the length of 2L and four propellers with an equal height h, which are located at the four corners of the robot's frame. Each manipulator of the robot is composed of two links and the links are connected to each other and to the main body of the robot by the revolute joints. As shown in Fig. 1, L_1 represent the length of the links AB and DE and L_2 represent the length of the links BC and EF. The joints axis is normal to the main body and in a plane. When the robot is in flight mode, it has 10-DOF. By increasing or decreasing the speed of the rotors and changing the torque of the

joints, various maneuvers can be performed. The ends of the two manipulators are constrained on a path. In this section, the dynamic equations of the quadrotor with two constrained manipulators are obtained.

As shown in Fig. 1, two basic coordinate frames are defined to describe the robot motion: earth fixed frame E = {X,Y,Z} and body fixed frame B = {x,y, z}. The origin of the body fixed frame is connected to the center of the main body.

Also, Euler angles 3-2-1, displayed respectively by ψ, θ, ϕ, are used to describe the orientation of the main body.

Thus, the rotation matrix of the main body is given as:

$$\mathbf{R}(\psi,\theta,\varphi)=\begin{bmatrix} C_\psi C_\Theta & S_\psi C_\Theta & -S_\Theta \\ S_\Theta S_\varphi C_\psi - C_\varphi S_\psi & S_\Theta S_\varphi S_\Psi + C_\varphi C_\psi & S_\varphi C_\Theta \\ S_\Theta C_\varphi C_\psi + S_\varphi S_\psi & S_\Theta C_\varphi C_\psi - S_\varphi S_\psi & C_\varphi C_\Theta \end{bmatrix} \quad (1)$$

where C and S stand for the cosine and sine, respectively. According to Fig. 1, the generalized coordinate vector (**q**) and the velocity coordinates (**η**) are chosen as:

$$\begin{aligned} \mathbf{q}&=\left((\mathbf{P}_o^E)^T,\boldsymbol{\gamma}^T,\boldsymbol{\alpha}^T\right)^T \\ &=(X,Y,Z,\varphi,\theta,\psi,\alpha_1,\alpha_2,\alpha_3,\alpha_4)^T \\ \boldsymbol{\eta}&=\left((\mathbf{v}_o^B)^T,(\boldsymbol{\omega}^B)^T,(\dot{\boldsymbol{\alpha}})^T\right)^T \\ &=\left(v_x,v_y,v_z,p,q,r,\dot\alpha_1,\dot\alpha_2,\dot\alpha_3,\dot\alpha_4\right)^T \end{aligned} \quad (2)$$

where $\mathbf{P}_o^E=(X,Y,Z)^T$, $\mathbf{v}_o^B=\left(v_x,v_y,v_z\right)^T$ and $\boldsymbol{\omega}^B=(p,q,r)^T$ are the position vectors of the origin (point O in Fig. 1) in frame E, the linear velocity vector of the body frame's origin and the angular velocity vector of the main body in frame B, respectively. Also, superscript B and E are the body and inertial frames, respectively; $\boldsymbol{\alpha}=\left(\alpha_1,\alpha_2,\alpha_3,\alpha_4\right)^T$ is the vector of joint angles. The inertial and body-fixed velocity relations are introduced as:

$$\begin{bmatrix}\mathbf{v}_o^B \\ \boldsymbol{\omega}^B\end{bmatrix}=\begin{bmatrix}\mathbf{R}(\gamma) & \mathbf{0} \\ \mathbf{0} & \mathbf{J}(\gamma)\end{bmatrix}\begin{bmatrix}\dot{\mathbf{P}}_o^E \\ \dot\gamma\end{bmatrix} \quad (3)$$

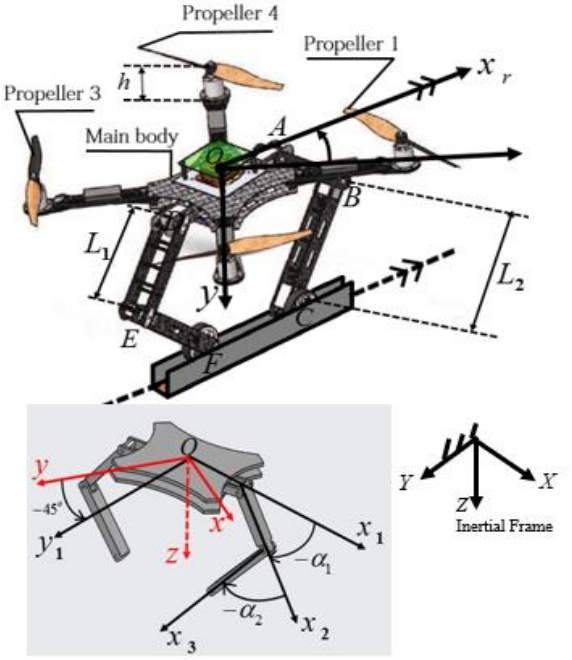

Fig. 1. A quadrotor with two manipulators and utilized frames.

where the Jacobian matrix J is given as follows:

$$\mathbf{J}(\boldsymbol{\gamma})=\begin{bmatrix}1 & 0 & -\sin\theta \\ 0 & \cos\varphi & \sin\varphi\cos\theta \\ 0 & -\sin\varphi & \cos\varphi\cos\theta\end{bmatrix} \quad (4)$$

The kinematic equations of the robot can be written as:

$$\boldsymbol{\eta}=\begin{bmatrix}\mathbf{R}(\gamma) & \mathbf{0} \\ \mathbf{0} & \mathbf{J}(\gamma) \\ & \mathbf{I}\end{bmatrix}\dot{\mathbf{q}}=\Theta\dot{\mathbf{q}} \quad (5)$$

Now, Lagrange method is used to obtain the dynamic equations of the robot in the flight mode [38]:

$$\frac{d}{dt}\left(\frac{\partial L}{\partial \eta}\right)+\frac{\partial L}{\partial \eta}\left[\left(\dot\Theta-\frac{\partial \eta}{\partial \mathbf{q}}\right)\Theta^{-1}\right]-\frac{\partial L}{\partial \mathbf{q}}\Theta^{-1}=\mathbf{U} \quad (6)$$

where L=T-P; T and P are the kinetic energy and the potential energy, respectively [37]. Also, U is the generalized force vector. Aerodynamic studies show that a drag moment and a thrust force are created by the rotation of each propeller [6]. The thrust force F and drag moment τ, are proportional to the square of propeller's angular velocity Ω which is given as:

$$F=k_t\Omega^2 \quad , \quad \tau=k_d\Omega^2 \tag{7}$$

where k_t and k_d are the thrust and drag moment constant coefficients, respectively. Therefore, the generalized force vector is given as:

$$\mathbf{U}=\mathbf{B}\boldsymbol{\tau}=\begin{pmatrix} 0 \\ 0 \\ -k_t\left(\Omega_1^2+\Omega_2^2+\Omega_3^2+\Omega_4^2\right) \\ -L\,k_t\left(\Omega_2^2-\Omega_4^2\right) \\ -L\,k_t\left(\Omega_3^2-\Omega_1^2\right) \\ -k_d\left(\Omega_1^2-\Omega_2^2+\Omega_3^2-\Omega_4^2\right) \\ \tau_1 \\ \tau_2 \\ \tau_3 \\ \tau_4 \end{pmatrix}=\begin{pmatrix} 0 \\ 0 \\ u_1 \\ u_2 \\ u_3 \\ u_4 \\ u_5 \\ u_6 \\ u_7 \\ u_8 \end{pmatrix} \tag{8}$$

where $\mathbf{B}\in R^{10\times 8}$ is the distribution of inputs matrix and τ_i (i=1,2,3,4) are the joint torques on the manipulators.

As shown in Fig. 1, the contact between the robot and constrained path is considered with the rollers in the points C and F. Frame $x^Ry^Rz^R$is defined on the constraint. In order to move along the constrained path, the speed of the points C and F along z_1 and $y_1$axes of $x^Ry^Rz^R$ frame should be zero. Therefore, the constraints are written as:

$$\begin{aligned} &\mathbf{V}_C^R\cdot\mathbf{k}^R=0\ ,\ \mathbf{V}_C^R\cdot\mathbf{j}^R=0 \\ &\mathbf{V}_F^R\cdot\mathbf{k}^R=0,\ \mathbf{V}_F^R\cdot\mathbf{j}^R=0 \\ &\omega^{\mathbf{R}}\cdot\mathbf{i}^R=0 \end{aligned} \tag{9}$$

where $\mathbf{i}^R$, $\mathbf{j}^R$and $\mathbf{k}^R$ are unit vectors in the direction of the x^R, y^R and z^R axes, respectively. The relations given in Eq. (9) are written in the matrix form as follows [38]:

$$\bar{\mathbf{A}}\,\dot{\mathbf{q}}=\mathbf{0} \tag{10}$$

where $\bar{\mathbf{A}}\in R^{5\times 10}$. Considering these five constraints, the dynamic equations of the constrained robot are written as follows [38]:

$$\mathbf{M}(\mathbf{q})\,\dot{\boldsymbol{\eta}}+\mathbf{h}(\mathbf{q},\boldsymbol{\eta})=\mathbf{B}\boldsymbol{\tau}+\mathbf{A}^T\boldsymbol{\lambda} \tag{11}$$

where $\mathbf{M}(\mathbf{q})\in R^{10\times 10}$is the mass matrix; $\mathbf{h}\in R^{10\times 1}$ is the centrifugal, Coriolis and gravity forces vector; $\mathbf{B}\in R^{10\times 8}$ is the input distribution matrix; $\boldsymbol{\tau}\in R^{\mathbf{8\times 1}}$ whose four first elements correspond to the propeller and four other elements are related to the torque of the robot joints; $\boldsymbol{\lambda}\in R^{5\times 1}$ is the Lagrange coefficients vector and $\mathbf{A}=\bar{\mathbf{A}}\,\mathbf{W}$ with $\mathbf{W}=\Theta^{-1}$.

3. Controller design

In this section, the robot is controlled in the presence of the external disturbances and uncertainty. At first, the control law is derived based on accurate dynamic model and then by estimating the nonlinear terms of the dynamic model, a robust adaptive controller is proposed.

3.1. Controller design based on accurate dynamic model

The robot has eight inputs and ten generalized coordinates. The five constraints of the system reduce the degree of freedom of the robot to five. Therefore, the reduced form equations can be obtained using the constraints. To this end, the dynamic equations of the constrained robot, Eq. (11), are rewritten in terms of $\mathbf{q}$, $\dot{\mathbf{q}}$. The second time derivative of Eq. (5) is written as:

$$\ddot{\mathbf{q}}=\dot{\mathbf{W}}\boldsymbol{\eta}+\mathbf{W}\dot{\boldsymbol{\eta}} \tag{12}$$

Substituting Eq. (5) into Eq. (12) yields:

$$\ddot{\mathbf{q}}=\dot{\mathbf{W}}\Theta\dot{\mathbf{q}}+\mathbf{W}\dot{\boldsymbol{\eta}} \tag{13}$$

Hence, the vector $\dot{\boldsymbol{\eta}}$ can be given as:

$$\dot{\boldsymbol{\eta}}=\mathbf{W}^{-1}\left(\ddot{\mathbf{q}}-\dot{\mathbf{W}}\Theta\dot{\mathbf{q}}\right) \tag{14}$$

By substituting Eq. (14) into Eq. (11) the dynamic equations are rewritten as follows:

$$\mathbf{M}\mathbf{W}^{-1}\left(\ddot{\mathbf{q}}-\dot{\mathbf{W}}\Theta\dot{\mathbf{q}}\right)+\mathbf{h}(\mathbf{q},\dot{\mathbf{q}})=\mathbf{B}\boldsymbol{\tau}+\mathbf{A}^T\boldsymbol{\lambda} \tag{15}$$

In order to obtain the reduced form of the dynamic equations, the vector of the generalized velocities is decomposed into constrained and non-constrained coordinates by the invertible matrix $\mathbf{P}$.

$$\dot{\mathbf{q}}=\mathbf{P}\begin{pmatrix}\dot{\mathbf{q}}_{\mathbf{c}}\\ \dot{\mathbf{q}}_{\mathbf{nc}}\end{pmatrix} \tag{16}$$

where, $\mathbf{q_{nc}}\in R^5$, $\mathbf{q_c}\in R^5$ are non-constrained and constrained coordinates, respectively and $\mathbf{P}\in R^{10\times10}$ is invertible. Also, since there are five constraints governing the system, five elements of vector $\dot{\mathbf{q}}$ are assigned to vector $\dot{\mathbf{q}}_{\mathbf{c}}$. Substituting Eq. (16) into Eq. (10) yields:

$$\mathbf{G}_1\dot{\mathbf{q}}_c+\mathbf{G}_2\dot{\mathbf{q}}_{nc}=\mathbf{0} \tag{17}$$

where $\mathbf{G}_1\in R^{5\times5}$and $\mathbf{G}_2\in R^{5\times5}$ are sub-matrices of $\bar{\mathbf{A}}\mathbf{P}$ determined by:

$$\bar{\mathbf{A}}\mathbf{P}=[\mathbf{G}_1 \quad \mathbf{G}_2] \tag{18}$$

By using Eq. (17), the vector $\dot{\mathbf{q}}_{\mathbf{c}}$is obtained in terms of $\dot{\mathbf{q}}_{nc}$.

$$\dot{\mathbf{q}}_c=-\mathbf{G_1}^{-1}\,\mathbf{G_2}\dot{\mathbf{q}}_{nc} \tag{19}$$

Hence, Eq. (16) is rewritten in terms of $\dot{\mathbf{q}}_{nc}$.

$$\dot{\mathbf{q}}=\mathbf{H}\,\dot{\mathbf{q}}_{nc} \tag{20}$$

where, the matrix $\mathbf{H}$ is defined as follows:

$$\mathbf{H}=\mathbf{P}\begin{pmatrix}-\mathbf{G_1}^{-1}\,\mathbf{G_2}\\ \mathbf{I}_{5\times5}\end{pmatrix} \tag{21}$$

Time derivative of Eq. (20) yields:

$$\ddot{\mathbf{q}}=\dot{\mathbf{H}}\,\dot{\mathbf{q}}_{nc}+\mathbf{H}\,\ddot{\mathbf{q}}_{nc} \tag{22}$$

By substituting Eq. (22) into Eq. (15), another form of the dynamical equations of the robot is obtained.

$$\mathbf{M}\mathbf{W}^{-1}\big(\dot{\mathbf{H}}\,\dot{\mathbf{q}}_{nc}+\mathbf{H}\,\ddot{\mathbf{q}}-\dot{\mathbf{W}}\Theta\dot{\mathbf{q}}\big)+\mathbf{h}(\mathbf{q},\boldsymbol{\eta})=\mathbf{B}\boldsymbol{\tau}+\mathbf{A}^{\mathrm{T}}\boldsymbol{\lambda} \tag{23}$$

Pre multiplying Eq. (23) by $\mathbf{H}^{\mathrm{T}}\mathbf{W}^{-\mathrm{T}}$, the reduced form equations are given as

$$\bar{\mathbf{M}}\ddot{\mathbf{q}}_{nc}+\bar{\mathbf{h}}=\bar{\mathbf{B}}\boldsymbol{\tau} \tag{24}$$

with

$$\begin{aligned}\bar{\mathbf{M}}&=\mathbf{H}^{\mathrm{T}}\mathbf{W}^{-1^{\mathrm{T}}}\mathbf{M}\mathbf{W}^{-1}\,\mathbf{H}\\ \bar{\mathbf{h}}&=\mathbf{H}^{\mathrm{T}}\mathbf{W}^{-1^{\mathrm{T}}}\begin{pmatrix}\mathbf{h}(\mathbf{q},\dot{\mathbf{q}})-\mathbf{M}\mathbf{W}^{-1}\dot{\mathbf{W}}\Theta\dot{\mathbf{q}}\\ +\mathbf{M}\mathbf{W}^{-1}\dot{\mathbf{H}}\dot{\mathbf{q}}_{nc}\end{pmatrix}\\ \bar{\mathbf{B}}&=\mathbf{H}^{\mathrm{T}}\mathbf{W}^{-1^{\mathrm{T}}}\mathbf{B}\end{aligned} \tag{25}$$

In Eq. (25), $\bar{\mathbf{A}}\mathbf{H}=\mathbf{0}$ has been used. Now, the controller is designed using the dynamic model (Eq. (25)). For this goal, the errors are defined as:

$$\mathbf{e}=\mathbf{q}_{nc}^{\mathbf{d}}-\mathbf{q}_{nc} \tag{26}$$

$$\boldsymbol{\sigma}=\dot{\mathbf{e}}+\mathbf{K}_1\mathbf{e} \tag{27}$$

where, $\mathbf{q_{nc}}$ shows the coordinates that are controlled. Superscript ‘d’ denotes the desired value and $\mathbf{K_1}$ is a constant positive definite diagonal matrix. Using the dynamic model (Eq. (24)), time derivative of Eq. (27) yields:

$$\dot{\boldsymbol{\sigma}}=\ddot{\mathbf{q}}_{nc}^{\mathbf{d}}+\mathbf{K_1}\dot{\mathbf{e}}-\bar{\mathbf{M}}^{-1}\bar{\mathbf{B}}\tau+\bar{\mathbf{M}}^{-1}\bar{\mathbf{h}} \tag{28}$$

Based on dynamic (Eq. (28)), the control law is suggested as follows:

$$\boldsymbol{\tau}=\bar{\mathbf{B}}^{-1}\bar{\mathbf{M}}(\mathbf{K_1}\dot{\mathbf{e}}+\ddot{\mathbf{q}}_{nc}^{d}+\mathbf{K}_2\,\boldsymbol{\sigma})+\bar{\mathbf{B}}^{-1}\bar{\mathbf{h}} \tag{29}$$

While the dynamic model is accurate, the error of dynamics is given as:

$$\dot{\boldsymbol{\sigma}}+\mathbf{K}_2\boldsymbol{\sigma}=0 \tag{30}$$

Considering the Lyapunov function $\mathbf{V}=\frac{1}{2}\boldsymbol{\sigma}^{\mathrm{T}}\boldsymbol{\sigma}$, its time derivative will be in the following form:

$$\dot{\mathbf{V}}=-\boldsymbol{\sigma}^{\mathrm{T}}\mathbf{K}_2\boldsymbol{\sigma} \tag{31}$$

Since $\mathbf{V}$ and $\dot{\mathbf{V}}$ are positive definite and negative definite, respectively, the tracking error converges to zero when $t\rightarrow\infty$. However, if the accurate dynamic model is not available, the controller (Eq. (29)) cannot be used and this is considered in the next sub-section.

3.2. Robust adaptive controller design

In this section, it is assumed that the Coriolis, centripetal, and gravity forces are not exactly modeled. Therefore, to compensate the dynamic model errors, the nonlinear terms of dynamic model are estimated by adaptive laws based on projection operator [39] and function approximation [40]. Therefore, in the proposed controller, the model nonlinear functions are not required to be known accurately, which is one of the main advantages of this controller.
To this end, the inputs are proposed as follows:

$$\boldsymbol{\tau}=\bar{\mathbf{B}}^{-1}\bar{\mathbf{M}}(\mathbf{K_1}\dot{\mathbf{e}}+\ddot{\mathbf{q}}^{d}_{nc}+\mathbf{K}_2\,\boldsymbol{\sigma})+\bar{\mathbf{B}}^{-1}\hat{\mathbf{h}} \tag{32}$$

where, $\hat{\mathbf{h}}$ is the estimation of $\bar{\mathbf{h}}$. Using the controller (Eq. (32)), the error of dynamics (Eq. (30)) is rewritten as:

$$\dot{\boldsymbol{\sigma}}+\mathbf{K}_2\boldsymbol{\sigma}=\bar{\mathbf{M}}^{-1}(\bar{\mathbf{h}}-\hat{\mathbf{h}}) \tag{33}$$

In order to determine $\hat{\mathbf{h}}$, the adaptive law is designed. To do so, let's define:

$$\begin{aligned}\mathbf{F}&=\bar{\mathbf{M}}^{-1}\mathbf{h}\\ \hat{\mathbf{F}}&=\bar{\mathbf{M}}^{-1}\hat{\mathbf{h}}\end{aligned} \tag{34}$$

where, $\hat{\mathbf{F}}$ is the estimation of $\mathbf{F}$. Functional approximation is used to estimate the vector elements of $\mathbf{F}$. For this purpose, $\mathbf{F}$ elements are approximated as temporal basic functions by constant weights. In other words,

$$\mathbf{F}_i=\mathbf{W}_i^{T}\mathbf{S}_i+\bar{\varepsilon}_i \qquad i=1,2,...,n_c \tag{35}$$

where, n_c is the number of coordinates under control and $\bar{\varepsilon}_i$ is the approximation error. $\mathbf{S}_i\in R^{\beta_i}$ and $\mathbf{W}_i\in R^{\beta_i}$ are basic functions and constant weights, respectively. Also, β_i is the number of basic functions. Estimation of elements $\mathbf{F}$ is considered as follows:

$$\hat{\mathbf{F}}_i=\hat{\mathbf{W}}_i^{T}\mathbf{S}_i \qquad i=1,2,...,n_c \tag{36}$$

where, $\hat{\mathbf{W}}_i$ is the estimation of $\mathbf{W}_i$. Since $\mathbf{W}_i$ is a constant vector, one can obtain an adaptive law using the Lyapunov function. For this purpose, the Lyapunov function is considered as:

$$\mathbf{V}=\frac{1}{2}\boldsymbol{\sigma}^{T}\boldsymbol{\sigma}+\frac{1}{2}\sum_{i=1}^{n_c}\tilde{\mathbf{W}}_i^{T}\Gamma_i^{-1}\tilde{\mathbf{W}}_i \tag{37}$$

where $\tilde{\mathbf{W}}_i=\mathbf{W}_i-\hat{\mathbf{W}}_i e$ is the estimation error. Time derivative of (Eq. (37)) during (Eq. (33)) yields:

$$\dot{\mathbf{V}}=-\boldsymbol{\sigma}^{T}\mathbf{K}_2\boldsymbol{\sigma}+\sum_{i=1}^{n_c}(\sigma_i\tilde{\mathbf{W}}_i^{T}\mathbf{S}_i-\tilde{\mathbf{W}}_i^{T}\Gamma_i^{-1}\dot{\hat{\mathbf{W}}}_i)+\boldsymbol{\sigma}^{T}\boldsymbol{\varepsilon} \tag{38}$$

Now, an adaptive law can be obtained for $\hat{\mathbf{W}}_i$ using (Eq. (38)). To this end, the projection operator for the adaptive law is proposed as follows:

$$\dot{\hat{\mathbf{W}}}_i=\text{proj}_{\Gamma_i}(\hat{\mathbf{W}}_i,\sigma_i\mathbf{S}_i,f_i) \quad i=1,2,...,n_c \tag{39}$$

where

$$\text{proj}_{\Gamma_i}=\begin{cases}\sigma_i\Gamma_i\mathbf{S}_i-\sigma_i\Gamma_i\mathbf{S}_i\dfrac{\nabla\mathbf{f}_i.\nabla\mathbf{f}_i^{T}}{\nabla\mathbf{f}_i^{T}.\nabla\mathbf{f}_i}\Gamma_i\mathbf{S}_i f_i & \text{if } f_i,\ a_i>0\\ \sigma_i\Gamma_i\mathbf{S}_i & \text{otherwise}\end{cases} \tag{40}$$

and $a_i=\sigma_i\mathbf{S}_i^{T}\Gamma_i\nabla\mathbf{f}_i$, $\nabla\mathbf{f}_i=\frac{\partial f_i}{\partial\hat{\mathbf{W}}}$, the functions f_i are convex functions that are considered as follows:

$$f_i=\frac{\|\hat{\mathbf{W}}_i\|^2-(\|\hat{\mathbf{W}}_i\|_M-\varepsilon_f)^2}{2\varepsilon_f\|\hat{\mathbf{W}}_i\|_M-\varepsilon_f^2} \tag{41}$$

where $\|\hat{\mathbf{W}}_i\|_M=\max(\|\hat{\mathbf{W}}_i\|)$. Note that for the projection operator defined in Eq. (40), the following inequality is true.

$$\begin{aligned}(\hat{\mathbf{W}}_i-\mathbf{W}_i)(\Gamma_i^{-1}\,&\text{proj}_{\Gamma_i}(\hat{\mathbf{W}}_i,\sigma_i\mathbf{S}_i,f_i)\\ &-\sigma_i\mathbf{S}_i)\le 0 \quad i=1,2,...,n_c\end{aligned} \tag{42}$$

Lavretsky et al. have presented more basic details for the projection operator [40]. Now, the following theorem is given for control of the considered robot.

Theorem 1: To control the constrained robot system with the dynamic Eq. (10 and 11), the control law (Eq. (32)) and the adaptive law (Eq. (39)) are proposed. These laws cause the robot to follow the reference trajectory in the presence of

the dynamic uncertainty, so that the tracking and estimation errors can be bounded.

Proof: Consider the Lyapunov function given in Eq. (37) and its time derivative Eq. (38). Using the control law (Eq. (32)), the adaptive laws (Eq. (39)) and inequality (Eq. (42)) yield:

$$\dot{\mathbf{V}} \leq -\boldsymbol{\sigma}^{T}\mathbf{K}_2\boldsymbol{\sigma} + \boldsymbol{\sigma}^{T}\boldsymbol{\varepsilon} \tag{43}$$

Now, the Yang inequality ($a, b \in R^2$, $\rho>0$ s.t $ab \leq \frac{1}{2}(\frac{a^2}{\rho}+\rho b^2)$) is used and Eq. (38) is rewritten as:

$$\dot{\mathbf{V}} \leq -\frac{1}{2}(\lambda_{min}(\mathbf{K}_2)\|\sigma\|^2 - \frac{\|\varepsilon\|^2}{\lambda_{min}(\mathbf{K}_2)}) \tag{44}$$

Using the Lyapunov function, Eq. (44) yields:

$$\dot{\mathbf{V}} \leq -\lambda_{min}(\mathbf{K}_2)\mathbf{V} + \rho \tag{45}$$

Solving Eq. (45) for V gives:

$$V(t) = V_0 e^{-\lambda_{min}(\mathbf{K}_2)t} + \frac{\rho}{\lambda_{min}(\mathbf{K}_2)}(1 - e^{-\lambda_{min}(\mathbf{K}_2)t}) \tag{46}$$

where $\rho = \frac{\|\varepsilon\|^2}{2\lambda_{min}(\mathbf{K}_2)}$. It shows $\mathbf{V}(t)$ will go to bounded value $\frac{\rho}{\lambda_{min}(\mathbf{K}_2)}$ when $t \to \infty$. Therefore, by choosing the gain values, this constant value can be tuned small. Thus, the tracking errors and uncertain estimations will be limited and the proof will be completed.

4. Simulation results

Here, the numerical simulation results of the robot motion under the proposed controller are presented. The robot parameters are given in Table 1.

The non-constrained and constrained coordinates are considered as follows:

$$\mathbf{q}_{n\,c} = (X, Z, \theta, \alpha_1, \alpha_3)^T$$
$$\mathbf{q}_c = (Y, \varphi, \psi, \alpha_2, \alpha_4)^T \tag{47}$$

Table 1. Physical parameters of the quadrotor [37].

Parameter	Value
m_b	1.13 kg
m_p	0.01 kg
m_{AB}	0.04 kg
m_{DE}	0.04 kg
m_{BC}	0.14 kg
m_{EF}	0.14 kg
L_{AB}	0.15 m
L_{DE}	0.15 m
L_{BC}	0.22 m
L_{EF}	0.22 m
h	0.03 m
L	0.5 m
k_d	2.1×10^{-5} N.s^2
k_t	2.1×10^{-5} N.s^2
I_{Xb}	1.27×10^{-2} kg.m^2
I_{yb}	1.27×10^{-2} kg.m^2
I_{Zb}	2.29×10^{-2} kg.m^2
I_{Zp}	3.8×10^{-8} kg.m^2
I_{x_1}	0.17×10^{-4} kg.m^2
I_{y_1}	0.17×10^{-4} kg.m^2
I_{z_1}	0.12×10^{-3} kg.m^2
I_{z_2}	0.12×10^{-3} kg.m^2
I_{x_2}	0.31×10^{-4} kg.m^2
I_{y_2}	0.31×10^{-4} kg.m^2

4.1. Initial conditions and desired trajectory

Since the robot is constrained, the initial conditions have to satisfy the constraints. In order to satisfy the constraints defined in Eq. (9), the initial generalized velocities are chosen zero. But for the initial generalized coordinates, initial configuration of the robot has to satisfy the holonomic constraints. To this end, the initial configuration of the robot is considered as Fig. 2(b). It is assumed that the center of the main body of the robot moves as much as d in the vertical direction from its highest possible point; and the main body rotates clockwise as much as β about y^R. Therefore, the rotation matrix defined in Eq. (1) can be obtained as Eq. (48).

$$\mathbf{R}(\psi,\theta,\varphi)=\frac{1}{2}\begin{bmatrix}1+C_\beta & 1-C_\beta & \sqrt{2}S_\beta\\ 1-C_\beta & 1+C_\beta & -\sqrt{2}S_\beta\\ -\sqrt{2}S_\beta & \sqrt{2}S_\beta & 2C_\beta\end{bmatrix} \quad (48)$$

The Eq. (48) yields:

$$\tan(\psi)=\frac{R_{12}}{R_{11}},\ \tan(\varphi)=\frac{R_{23}}{R_{33}}$$
$$\tan(\theta)=\frac{-R_{13}}{\sqrt{R_{11}^2+R_{12}^2}} \quad (49)$$

Thereby, ψ,θ and φ are obtained.
Now, $\alpha_i(i=1,2,3,4)$ should be determined. To this end, Eq. (50) can be obtained from Fig. 2.

$$\overrightarrow{OF}_z=\overrightarrow{OC}_z=L_{AB}+L_{BC}, \quad (50)$$

where, $(\dot{\cdot})_z$ denotes z component. Eq. (50) has two constraints; therefore, two variables are chosen and two others are obtained from Eq. (50). To, this end, α_2 and α_4 are chosen zero and α_1 and α_3 are determined by Eq. (50). It should be noted that the distance d' has to satisfy Eq. (51).

$$d'=d-\left(\frac{L}{\sqrt{2}}\right)\sin\beta\geq 0 \quad (51)$$

Therefore, by considering $\beta=4^0$ and d=4 cm, the value $d'=2.7680$ cm will be determined and by the rotation matrix, Euler angles are given as $\varphi=-2.8273^0$ and $\theta=-2.8273^0$ and $\psi=-0.0699^0$. Also, $\mathbf{P}_o^E$ is determined by defining the position Ó in initial frame and given as $\mathbf{P}_o^E=(0\ ,0\ ,0.04)^T$.

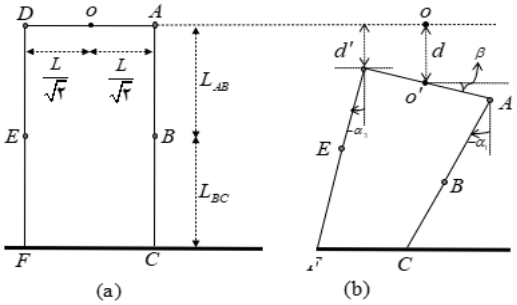

Fig. 2. (a) The robot configuration in the highest point on the path and (b) the initial configuration of the robot on the path.

Accordingly, the initial configuration of the robot is considered as Eq. (52).

$$\mathbf{P}_o^E=(0\ ,0,\ 0.04)^T$$
$$\gamma_0=(-2.8307^o,\ -2.8273^o,0.0699^o)^T \quad (52)$$
$$\alpha_0=(55.5125^o\ ,0,\ 55.5125^o,\ 0)^T$$

Since the constraint path is along the x_r axis, the desired path of the robot is defined as:

$$^R X_o^d(t)=\begin{cases}0.25t^2 & 0\leq t<12\\ 6\ t-36 & 12\leq t<20\\ -0.5t^2+26t-236 & 20\leq t<26\\ 102 & 26\leq t<30\\ -2t+162 & 30\leq t<80\end{cases} \quad (53)$$

For this path, the robot movement includes acceleration movement, constant velocity, deceleration, and fixed position during forward motion. Also, it moves with constant velocity during the way back.
It is assumed that this quadrotor has to monitor the path defined in Eq. (53). For this purpose, the robot posture is chosen as constant during motion. Therefore, the desired trajectory is given as in Eq. (54).

$$\mathbf{q}_{nc}^d=\begin{pmatrix}\frac{\sqrt{2}}{2}\left(^R X_o^d(t)\right)\\ 0.04\\ -\ 2.8273^o\\ 85^o\\ 85^o\end{pmatrix} \quad (54)$$

4.2. Performance of robust adaptive control

Now, the implementation results of the proposed adaptive controller are presented. It should be noted that this controller does not require to accurately know the dynamic model of the nonlinear functions. In the following, the ability of this controller for tracking the desired path (Eq. (54)) is investigated by the gains.

$$\mathbf{K}_1=\text{diag}([0.1,4.0,0.5,0.6,0.8])$$
$$\mathbf{K}_2=\text{diag}([0.02,70.02,18.55,82.0,75.2]) \quad (55)$$

The adaptive parameters are considered as $\varepsilon_i=0.1$, $\Gamma_i=\mathbf{I}_{\beta_i}$, $\|\Phi_i\|_M=1(i=1,...,5)$.

Fig. 3 shows the position of the main body in the $x^R y^R z^R$ frame. The desired path is specified with the dotted lines. As it can be seen, the controller without knowing the nonlinear terms of the dynamic model has forced the robot to move along the desired path. Also, according to the constraints (Eq. (9)), the robot has not moved along Y_o^R axis.

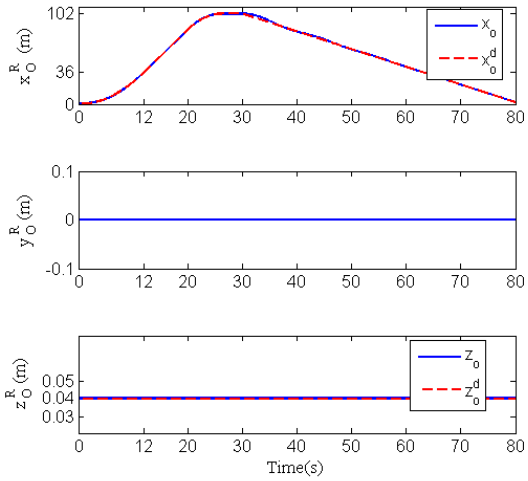

Fig. 3. Tracking performance of the quadrotor.

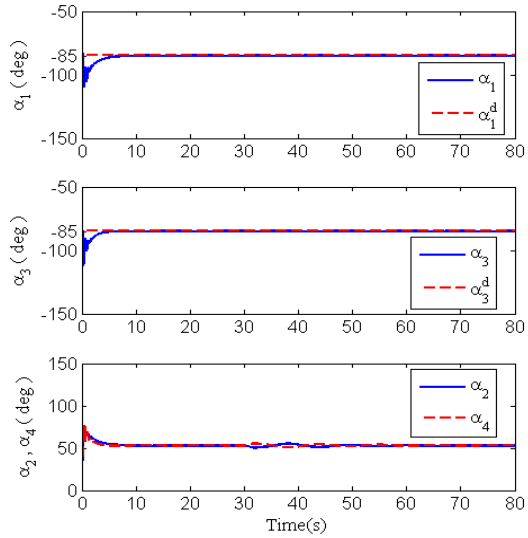

Fig. 4. The joint angles of the manipulators during quadrotor motion

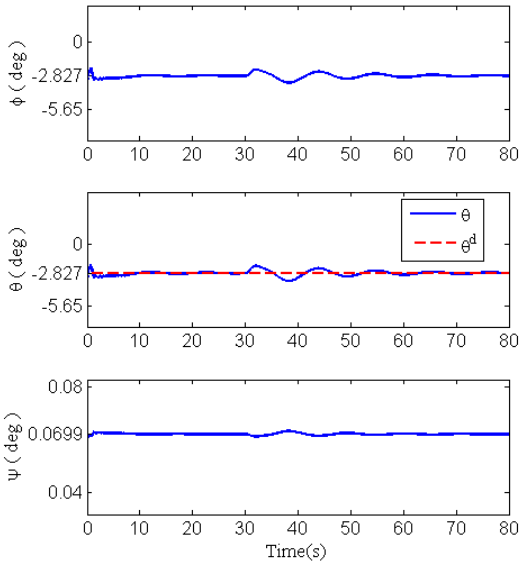

Fig. 5. Euler angles during quadrotor motion.

The joint angles are shown in Fig. 4. The angles α_1 , α_3 reach the desired value in less than one second from the start of the movement. Also, the angles α_2 and α_4 converge to a constant value of 58.4 degrees.

Euler angles are shown in Fig. 5. As expected, the angle θ is well controlled and two other angles remain constant.

The control inputs are shown in Fig. 6. Due to the fact that Euler's angles are constant, the roll, pitch and yaw moments are zero. As seen from Fig. 6, input u_1, the lift force, has nonzero value during accelerated motion. The joint torques are shown in Fig. 7. It is seen that torques are bounded during motion. It is obvious that during the movement without acceleration, the joint torques are nonzero as the lift force (u_1) is almost zero and this means that the robot weight is controlled by the joint torques during the movement without acceleration.

In Fig. 8, the estimated values of nonlinear terms in dynamic model are shown and compared with their actual values. This figure shows that the estimation error is bounded during motion. Therefore, these results show that the constrained quadrotor can follow the reference trajectory by the proposed adaptive control in spite of the dynamic model uncertainty.

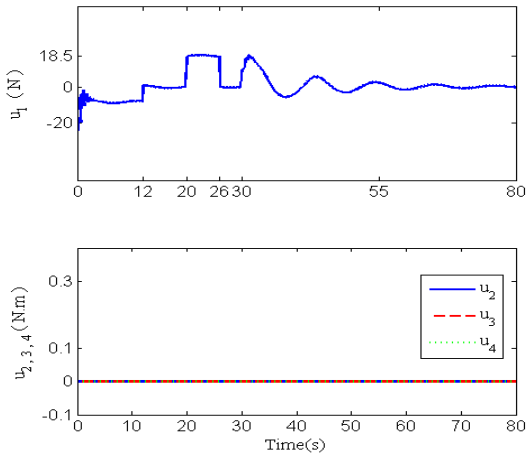

Fig. 6. The control inputs u_1, u_2, $u_3$and u_4 during quadrotor motion

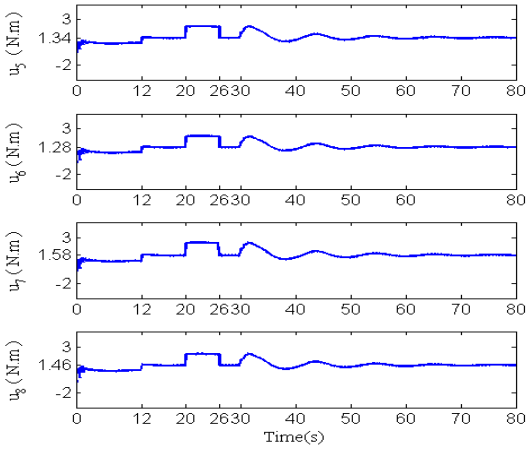

Fig. 7. The joint torques during quadrotor motion.

4.3. Performance of robust adaptive controller in presence of external disturbances

In this section, robust control of the robot is investigated in the presence of the wind force as the external disturbance. It is assumed that the wind force 1.0N is applied from t=5 s by t=25 s along the x^R and y^R axes with the desired trajectory defined in Eq. (54). Fig. 9 shows the tracking performance of the quadrotor during motion by the adaptive parameters ε_i=0.1 , $\Gamma_i=\mathbf{I}_{\beta_i}$, $\|\Phi_i\|_M$=1(i=1,...,5). Fig. 9 shows that the proposed controller can force the quadrotor to move near the reference motion in spite of the dynamic model uncertainties and external disturbances.

The control inputs and joint torques are shown in Fig. 10 and 11, respectively. The effect of the external disturbances is manifest at 5 ≤t≤ 25 and the input values are limited in spite of the presence of the external disturbance and the dynamic uncertainties.

In Fig. 12, the estimated values of nonlinear terms of the dynamic model are shown and compared with their actual values.

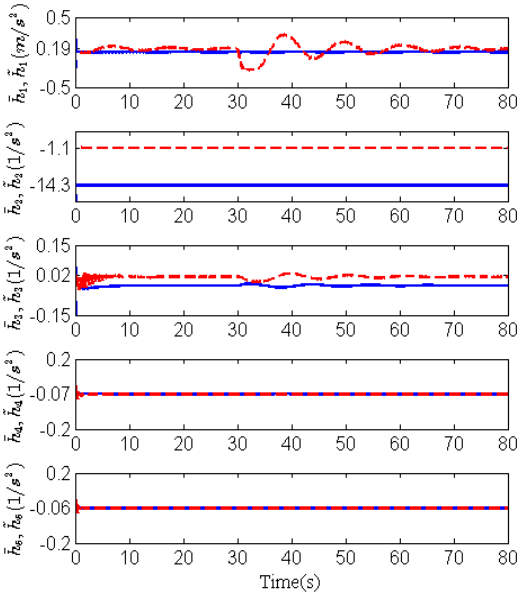

Fig. 8. Actual and estimated nonlinear terms, solid lines show the actual values and dash line shows the estimated values.

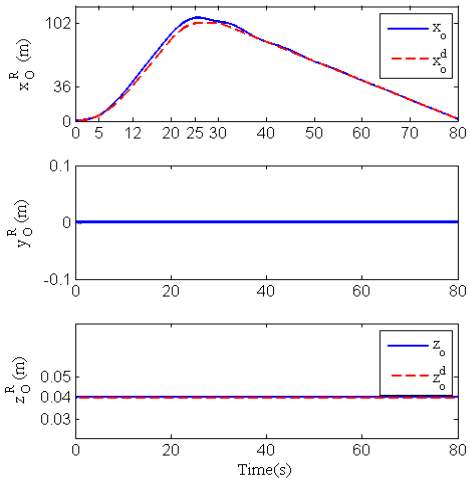

Fig. 9. Tracking performance of the quadrotor in presence of the external disturbance.

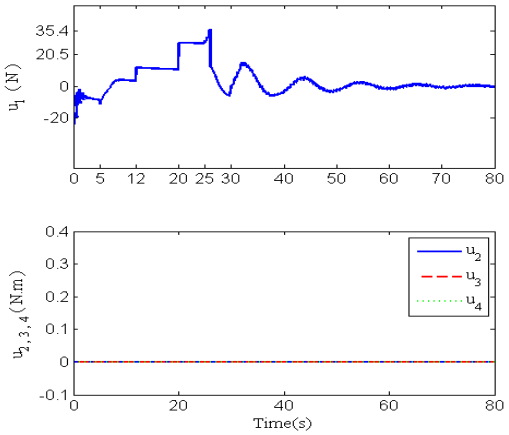

Fig. 10. The control inputs u_1, u_2, $u_3$and u_4 during quadrotor motion in presence of the external disturbance

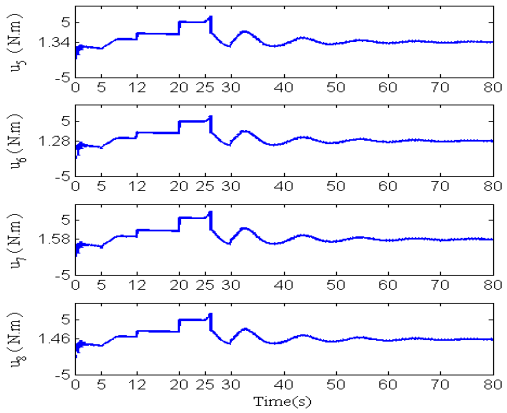

Fig. 11. The joint torques during quadrotor motion

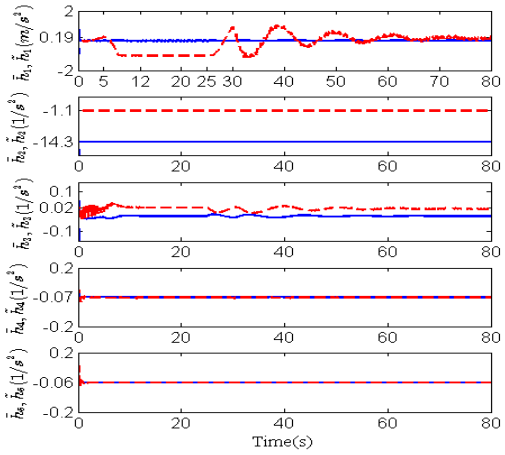

Fig. 12. Actual and estimated nonlinear terms in dynamic model in the presence of the external disturbance, solid lines show the actual values and dash line shows the estimated values.

5. Conclusions

A quadrotor with two constrained manipulators was introduced and controlled on a constraint path in the presence of dynamic uncertainties. By adding two manipulators to quadrotor and moving the robot on the constraint path, the under-actuated robot becomes over-actuated and one can use this feature to accurately control the position of the robot. A robust adaptive method was presented to control the robot. In the proposed method, the nonlinear terms of the dynamic model were estimated by adaptive laws based on functional approximation technique and projection operator. Numerical implementation results showed that the quadrotor can move near the reference path in the presence of the dynamic uncertainties by the proposed controller. Also, the robustness of the presented control is evaluated by surveying its performance in the presence of the wind force. The results showed that the proposed controller can move the quadrotor near the reference path in spite of the dynamic uncertainties and external disturbances.

References

[1] H. Wang, J. Shi, J. Wang, H. Wanget, Y. Feng and Y. You, "Design and Modeling of a Novel Transformable Land/Air Robot", *Int. J. Aerosp. Eng.*, Vol. 2019, ID: 2064131, pp. 1–10, (2019).

[2] S. Sadr, S. Ali A. Moosavian and P. Zarafshan, "Dynamics Modeling and Control of a Quadrotor with Swing Load", *J. Control Sci. Eng.*, Vol. 2014, ID: 265897, pp. 1–12, (2014).

[3] D. Nguyen, Y. Liu and K. Mori, "Experimental Study for Aerodynamic Performance of Quadrotor Helicopter", *Trans. Japan Soc. Aero. Space Sci.*, Vol. 61, No. 1, pp. 29–39, (2018).

[4] K. Nonami, "Drone technology, cutting-edge drone business, and future prospects", *J. Robot. Mechatron.*, Vol. 28, No. 3, pp. 262-272, (2016).

[5] A. Bousbaine, M. H. Wu and G. T. Poyi, "Modelling and simulation of a quad-rotor helicopter", *6th IET Int. Conf.*

Power Electron. Mach. Drives, Bristol, pp. 1–6, (2012).

[6] A. Najm and I. Ibraheem, "Nonlinear PID controller design for a 6-DOF UAV quadrotor system", *Eng. Sci. Technol. Int. J.*, Vol. 22, No. 4, pp. 1087–1097, (2019).

[7] M. Haemers, S. Derammelaere, C. M. Ionescu, K. Stockman, J. D. Viaene and F. Verbelen, "Proportional-Integral State-Feedback Controller Optimization for a Full-Car Active Suspension Setup using a Genetic Algorithm", *IFAC Pap. OnLine*, Vol. 51, No. 4, pp. 1-6, (2018).

[8] M. F. Bin Abas, D. Pebrianti, S. A. Md. Ali, D. Iwakura, Y. Song, K. Nonami and D. Fujiwara, "Circular Leader-Follower Formation Control of Quad-Rotor Aerial Vehicles", *J. Robot. Mechatron.*, Vol. 25, No. 1, pp. 60-71, (2012).

[9] Y. Y. Nazaruddin, A. D. Andrini and B. Anditio, "PSO Based PID Controller for Quadrotor with Virtual Sensor", *IFAC Pap. OnLine*, Vol. 51, No. 4, pp. 358-363, (2018).

[10] M. S. Chehadeh and I. Boiko, "Design of Rules for In-Flight Non-Parametric Tuning of PID Controllers for Unmanned Aerial Vehicles", *J. Franklin Inst.*, Vol. 356, No. 1, pp. 474-491, (2018).

[11] Y. Bouzid, H. Siguerdidjane and Y. Bestaoui, "Boosted Flight Controller for Quadrotor Navigation under disturbances", *IFAC Pap. OnLine*, Vol. 50, No. 1, pp. 10293-10298, (2017).

[12] Z. Yaou, W. jingsong, L. Tiansheng and L. Jingsong, "The attitude control of the four-rotor unmanned helicopter based on feedback linearization control", *WSEAS Trans. Syst.*, Vol. 12, No. 4, pp. 229-239, (2013).

[13] M. A. Lotufo, L. Colangelo, C. P. Montenegro, C. Novara and E. Canuto, "Embedded Model Control for UAV Quadrotor via Feedback Linearization", *IFAC Pap. OnLine*, Vol. 49, No. 17, pp. 266-271, (2016).

[14] D. Lee, H. J. Kim and S. Sastry, "Feedback linearization vs. adaptive sliding mode control for a quadrotor helicopter", *Int. J. Control Autom. Syst.*, Vol. 7, No. 3, pp. 419-428, (2009).

[15] K. Nonaka and H. Sugizaki, "Integral Sliding Mode Altitude Control for a Small Model Helicopter with Ground Effect Compensation", *Am. Control Conf.*, San Francisco, CA, USA, pp. 202–207, (2011).

[16] G. Alizadeh and K. Ghasemi, "Control of Quadrotor Using Sliding Mode Disturbance Observer and Nonlinear H∞", *Int. J. Rob.*, Vol. 4, No. 1, pp. 38-46, (2015).

[17] R. Akbar, B. Sumantri, H. Katayama, S. Sano, and N. Uchiyama, "Reduced-Order Observer Based Sliding Mode Control for a Quad-Rotor Helicopter", *Int. J. Rob. Mechatron.*, Vol. 28, No. 3, pp. 304-313, (2016).

[18] D. Ma, Y. Xia, G. Shen, Z. Jia and T. Li, "Flatness-based adaptive sliding mode tracking control for a quadrotor with disturbances", *J. Franklin Inst.*, Vol. 355, No.14, pp. 6300-6322, (2018).

[19] M. A. Mohd Basri, A. R. Husain and K. A. Danapalasingam, "Enhanced Backstepping Controller Design with Application to Autonomous Quadrotor Unmanned Aerial Vehicle", *J. Intell. Rob. Syst.*, Vol. 79, No. 2, pp. 295–321, (2014).

[20] Y. Liu, J. Ma and H. Tu, "Robust Command Filtered Adaptive Backstepping Control for a Quadrotor Aircraft", *J. Control Sci. Eng.*, Vol. 2018, ID: 1854648, pp. 1-9, (2018).

[21] M. A. Vallejo-Alarcon, R. Castro-Linares and M. Velasco-Villa, "Unicycle-Type Robot & Quadrotor Leader-Follower Formation Backstepping Control", *IFAC Pap. OnLine*, Vol. 48, No. 19, pp. 51-56, (2015).

[22] K. Djamel, M. Abdellah and A. Benallegu, "Attitude Optimal Backstepping Controller Based Quaternion for a UAV", *Math. Probl. Eng.*, Vol. 2016, ID: 8573235, pp. 1-11, (2016).

[23] S. Nadda and A. Swarup, "Development of backstepping based sliding mode control for a quadrotor", *IEEE 10th Int. Colloq. Signal Process. Appl.*, Kuala Lumpur, Malaysia, pp. 10-13, (2014).

[24] P. Sanchez-Cuevas, G. Heredia and A. Ollero, "Characterization of the Aerodynamic Ground Effect and Its Influence in Multirotor Control", *Int. J. Aerosp. Eng.*, Vol. 2017, ID: 1823056, pp. 1-17, (2017).

[25] M. Tognon, A. Testa, E. Rossi and A. Franchi, "Takeoff and Landing on Slopes via Inclined Hovering with a Tethered Aerial Robot", *IEEE/RSJ Int. Conf. Intell. Rob. Syst. (IROS)*, Daejeon, Korea (South), pp. 1-6, (2016).

[26] M. Muller, S. Lupashin and R. D. Andrea, "Quadrocopter ball juggling", *IEEE/RSJ Int. Conf. Intell. Rob. Syst. (IROS)*, San Francisco, CA, USA, pp. 5113-5120, (2011).

[27] C. Masone, H. Bulthoff and P. Stegagno, "Cooperative transportation of a payload using quadrotors: A reconfigurable cable-driven parallel robot", *IEEE/RSJ Int. Conf. Intell. Rob. Syst. (IROS)*, Daejeon, Korea (South), pp. 5113-5120, (2016).

[28] J. Gimenez, L. R. Salinas, D. C. Gandolfo, C. D. Rosales and R. Carelli, "Control for cooperative transport of a bar-shaped payload with rotorcraft UAVs including a landing stage on mobile robots", *Int. J. Syst. Sci.*, Vol. 51, No. 16, pp. 3378-3392, (2020).

[29] S. Lupashin, A. Schollig, M. Sherback, R. D. Andrea, "A simple learning strategy for high-speed quadrocopter multi-flips", *IEEE Int. Conf. Rob. Autom.*, Anchorage, AK, USA, pp. 1642-1648, (2010).

[30] D. Mellinger, N. Michael and V. Kumar, "Trajectory generation and control for precise aggressive maneuvers with quadrotors", *Int. J. Rob. Res.*, Vol. 31, No. 5, pp. 664-674, (2010).

[31] Y. Zou and Z. Meng, "Coordinated trajectory tracking of multiple vertical take-off and landing UAVs", *Autom.*, Vol. 99, pp. 33-40, (2019).

[32] F. Cakici and M. K. Leblebicioglu, "Control System Design of a Vertical Take-off and Landing Fixed-Wing UAV", *IFAC Pap. OnLine*, Vol. 49, No. 3, pp. 267-272, (2016).

[33] B. Michini, J. Redding, N. K. Ure, M. Cutler and J. P. How, "Design and flight testing of an autonomous variable-pitch quadrotor", *IEEE Int. Conf. Rob. Autom*, Shanghai, China, pp. 2978-2979, (2011).

[34] X. Ding , Y. Yu and J. J. Zhu, "Trajectory linearization tracking control for dynamics of a multi-propeller and multifunction aerial robot – MMAR", *IEEE Int. Conf. Rob. Autom.*, Shanghai, China, pp. 757-762, (2011).

[35] X. Ding and Y. Yu, "Dynamic Analysis, Optimal Planning and Composite Control for Aerial Arm-operating with a Multi-propeller Multifunction Aerial Robot", *IEEE Int. Conf. Rob. Autom*, Chengdu, China, pp. 420-427, (2012).

[36] X. Ding and Y. Yu, "Motion planning and stabilization control of a multi-propeller multifunction aerial robot", *IEEE/ASME Trans. Mechatron.*, Vol. 18, No. 2, pp. 645-656, (2013).

[37] X. Ding and Y. Yu, "On hybrid modeling and control of a multi-propeller multifunction aerial robot with flying-walking locomotion", *Auton. Rob.*, Vol. 38, No. 3, pp. 225–242, (2015).

[38] H. Baruh, *Analytical dynamics*, Boston: WCB/McGraw-Hill, pp. 421–481 (1999).

[39] R. Dehghani and H. M. Khanlo, "A regressor-free robust adaptive controller for autonomous underwater vehicles", *Proc. Inst. Mech. Eng., Part M: J. Eng. Marit. Environ.*, Vol. 231, No. 2, pp. 569-582, (2016).

[40] Z. Cai, M. S. de Queiroz and D. M. Dawson, "A sufficiently smooth projection operator", *IEEE Trans. Autom. Control*, Vol. 51, No. 1, pp. 135-139, (2006).

How to cite this paper:

M. Mohammadi, R. Dehghani and A.R. Ahmadi, "Robust adaptive projection-based control of a constrained quadrotor with two manipulators,", *J. Comput. Appl. Res. Mech. Eng.*, Vol. 11, No. 2, pp. 351-364, (2022).

DOI: 10.22061/JCARME.2021.5860.1741

URL: https://jcarme.sru.ac.ir/?_action=showPDF&article=1590